

Physicochemical Characterization of Nanohydroxyapatite Powder in Simulated Body Fluid Immersion: A Pilot Study

Nadhia Anindhita Harsas¹, Viona Yosefa², Maria Savvyana², Basril Abbas³, Endang Winiati Bachtiar⁴, Yuniarti Soeroso^{1*}

¹Department of Periodontology, Faculty of Dentistry, Universitas Indonesia, Jakarta, Indonesia

²Postgraduate student of Department of Periodontology, Faculty of Dentistry, Universitas Indonesia, Jakarta, Indonesia

³National Research and Innovation Agency (BRIN) Jakarta, Indonesia

⁴Department of Oral Biology, Faculty of Dentistry, Universitas Indonesia, Jakarta, Indonesia

Received 5 December 2022, Revised 13 March 2023, Accepted 20 April 2023

ABSTRACT

Nanohydroxyapatite (n-HA) has been widely used as a bone graft material. In contact with biological fluids, n-HA should be reactive, resorbable, form an bone-like apatite layer on their surfaces, and enhance osseointegration. The release of Ca, P, and O in SBF predicted the formation of bone-like apatite layer. Therefore, this study aims to investigate the physicochemical properties of nano-HA powder during the SBF immersion in vitro. The n-HA powder was immersed in SBF for 24, 48 hours, 7, 14, and 28 days. The swelling ratio, pH, FTIR, and SEM-EDX were analyzed pre- and post-SBF immersion. The n-HA powder showed excellent hydrophilicity and a stable pH, even though there was a pH decrease in 28 days. The carbonate and phosphate functional groups were found through FTIR, in line with the ion composition changes and increase of the Ca/P ratio shown on EDX. Both mean weight percentages (%) of Ca and P increased during 14 days of SBF immersion (16.15 to 27.27; and 8.57 to 11.68, respectively). The other functional groups on the n-HA are PO₃⁻, CO₂⁻, O-H, C=H, and COO. In conclusion, the n-HA powder presents good physicochemical properties that indicate the formation of an apatite bonelike layer and is promising as a bone graft material.

Keywords: nanohydroxyapatite; simulated body fluid; apatite bonelike; bone graft

1. INTRODUCTION

Bone is a combination of collagen fibrils as an organic phase with embedded nano-crystalline rod-like shaped inorganic materials[1], [2] The clinical need to promote the regeneration of bone defects due to chronic diseases such as periodontitis or trauma has agitated the development of bone grafting materials. Nowadays, bone grafting materials are divided into four categories based on their biological origins: autografts, allografts, xenografts, and alloplastic.[3] Autografts harvested from the host are still considered the gold standard but have some drawbacks, such as creating morbidity in the donor site and limiting quantity[2], [4] Allografts and xenografts may show an immune or allergic response tendency due to their origins in other humans or different species. Alloplastics as synthetic materials offer unlimited resources and minimize the risk of immunologic responses and transmissible diseases.[3]

* Corresponding author: yuniarti_22@yahoo.co.id

Hydroxyapatite (HA) is the main constituent of the mineral part of bone and teeth, with a general formula of $\text{Ca}_{10}(\text{OH})_2(\text{PO}_4)_6$, which represents 60–70% and 90% of the weight of bone and enamel, respectively.[1], [5], [6] The increased interest in synthetic HA has led to extensive research due to the chemical similarity of HA to natural bone. The advantages of synthetic HA are its biocompatibility, osteoconductive nature, and capability to bind to both hard and soft tissues. Hydroxyapatite, either in pure form or as composites, is non-inflammatory, non-toxic, and non-immunogenic and can form direct bonds with hard and soft tissues.[7] The disadvantage of HA is the length of time it degrades in the biological environment. The use of nanoscales is gaining interest due to their improved properties, such as surface effect, size, and quantum.

Nano-hydroxyapatite (n-HA) can provide the required amount of phosphate and calcium for the remineralization of human hard tissue, such as bone and tooth enamel. Other trace elements that have beneficial effects on the bioregeneration properties of the materials are Mg^{2+} , Sr^{2+} , Si^{4+} , Na^+ , and K^+ . [8], [9] Although nano-sized material is a promising application in dentistry, including for hard and soft tissue regeneration purposes, the study of nanoparticles is not new. The concept of the nanometer was first introduced by Richard Zsigmondy in 1925, and Richard Feynman introduced modern nanotechnology in 1959.[10] Dimensions of nanomaterials range from 1-100 nm, and in dentistry, the crystals range in size between 50 and 1000 nm.[5], [6] Nano-hydroxyapatite comes in several forms, including spherical, cubic, and needle-like nanoscale particles. Nanomaterials also showed the ability to form components autonomically without human intervention.[11], [12]

An indicator of a material's bonding with bone is the development of a biologically active bone-like apatite layer on its surface. Nano-hydroxyapatite can be reactive, resorb, and form a bone-like apatite on their surfaces; it is known that n-HA can stimulate osseointegration.[13] The biomineralization of apatite on bioactive ceramic is a self-remodeling process by bone cells and proteins and appears to be initiated by the blood plasma.[14] This *in vivo* apatite bonelike formation can be reproduced *in vitro* using simulated body fluid (SBF) with ion concentrations nearly equal to those in blood plasma.[14], [15] The ability to develop this apatite bone-like formation has been known as bioactivity and is influenced by the material's chemical, microstructure, and surface features. Apatite bonelike layer formation also depends on several characteristics of the liquid environment, such as pH, ionic strength, supersaturation, and temperature. [13]

The formation of the apatite layer in SBF is used only as an initial indication to see the potential of a biomaterial. There are several limitations on using SBF on evaluate the formation of a bonelike apatite layer *in vitro*. First, no protein plays a role in apatite nucleation, the second is the presence of tris hydroxymethyl-aminomethane to control the pH of SBF, and finally, there is no control over the carbonate contained in SBF.[16] But, despite the limitations, SBF remained a potential instrument to predict *in vivo* bone-bonding ability.

The bioactivity of n-HA occurs when an apatite layer is formed due to the presence of PO_4^{3-} , and Ca^{2+} ions. The concentration of calcium, phosphorus, and other ions may indicate the structure of newly formed hydroxyapatite. Scanning Electron Microscope - Energy Dispersive Spectroscopy (SEM-EDX) can display high-resolution bonelike apatite layer formation images with magnification up to 20.000 times. It is also used to analyze the composition of the hydroxyapatite layer that formed after the immersion by measuring the concentration of inorganic ions in a bone structure such as calcium, sodium, magnesium, and others. Chemical properties in this study were analyzed by Fourier transform

infrared (FTIR) to identify the formation of an apatite layer on the materials after SBF immersion.[13]

The powder form of n-HA is commonly used to reconstruct periodontal bone defects. This powder form also provides easy manipulation and can be used as a base material combined with other polymers to create composites to increase their properties that support regeneration. Therefore, this present study attempts to investigate the physicochemical properties of nano-HA powder through in vitro bioactivity. An experimental in vitro study was performed by immersing n-HA powder in an SBF at a controlled temperature. The hydrophilicity of n-HA powder and pH changes were observed over time of SBF immersion. For a better understanding of bonelike apatite layer formation, scaffold morphology, chemical composition, and crystalline structure, FTIR and SEM-EDX analyses were used.

2. MATERIALS AND METHODS

2.1 Nanohydroxyapatite (n-HA) powder preparation

Nano-hydroxyapatite (n-HA) powder was prepared in the National Research and Innovation Agency (BRIN) Jakarta, Indonesia. Samples were prepared by reacting calcium hydroxide ($\text{Ca}(\text{OH})_2$) with phosphoric acid (H_3PO_4) using the precipitation reaction method. Suspension of $\text{Ca}(\text{OH})_2$ 0.5 molar was prepared using powdered calcium hydroxide (Merck, Germany) with purified water. The suspension was degassed by stirring at 40 °C at 200 rpm for two hours. A solution of phosphoric acid (H_3PO_4) 0.3 molar (Merck, Germany) was added dropwise (50 drops/min) into the $\text{Ca}(\text{OH})_2$ suspension while stirring with a magnetic stirrer at 200 rpm until the H_3PO_4 solution was used up, resulting in a hydroxyapatite slurry. The pH during the process was adjusted to about 9 with an ammonium hydroxide solution and stirred for 1 hour. Sodium bicarbonate (NaHCO_3) 8.4 g (0.1 M) was added to the HA slurry while stirring with a magnet at 200 rpm. After dissolved NaHCO_3 , stirring was continued for 1 hour, then sonicated for 2 hours. The slurry of HA carbonation was left for 20 hours, then filtered through a Buchner filter. The precipitate was dried at 60 °C for 24 hours, then heated at 100 °C for 7200 s.

2.2 Simulated Body Fluid (SBF) preparation

Simulated body fluid (SBF) was prepared in the laboratory of chemistry, Faculty of Medicine, Universitas Indonesia. The SBF has ion concentrations nearly equal to those of human blood plasma (Table 1). The number of reagent-grade chemicals was prepared using Kokubo's Protocol to prepare the SBF.[17] Sodium chloride (NaCl), sodium hydrogen carbonate (NaHCO_3), potassium chloride (KCl), dipotassium hydrogen phosphate ($\text{K}_2\text{HPO}_4 \cdot 3\text{H}_2\text{O}$), magnesium chloride hexahydrate ($\text{MgCl}_2 \cdot 6\text{H}_2\text{O}$), calcium chloride dihydrate ($\text{CaCl}_2 \cdot 2\text{H}_2\text{O}$), sodium sulfate (Na_2SO_4) and tris-hydroxymethyl aminomethane ($(\text{HOCH}_2)_3\text{CNH}_2$). Aquabidestilata was poured into a polypropylene beaker and stirred at 36.5 °C. NaCl , KCl , $\text{K}_2\text{HPO}_4 \cdot 3\text{H}_2\text{O}$, $\text{MgCl}_2 \cdot 6\text{H}_2\text{O}$, CaCl_2 , and Na_2SO_4 were dissolved into Tris and buffered to pH 7.40 at 36,5 °C with hydrochloric acid.

Table. 1 Comparison of Ion Concentrations between Simulated Body Fluid and Blood Plasma

Ion	Concentration 10^{-3} mol	
	SBF (pH 7.4)	Blood plasma (pH 7.2-7.4)
Na^+	142.0	142.0
K^+	5.0	5.0
Mg^{2+}	1.5	1.5

Ion	Concentration 10^{-3} mol	
	SBF (pH 7.4)	Blood plasma (pH 7.2-7.4)
Ca ²⁺	2.5	2.5
Cl ⁻	147.8	103.0
HCO ₃ ⁻	4.2	27.0
HPO ₄ ³⁻	1.0	1.0
SO ₄ ²⁻	0.5	0.5

Table. 2 Chemical Composition of the Simulated Body Fluid

Order	Reagent	Amount
1	NaCl	7.996 g
2	NaHCO ₃	0.350 g
3	KCl	0.224 g
4	K ₂ HPO ₄ .3H ₂ O	0.228 g
5	MgCl ₂ .6H ₂ O	0,305 g
6	1M-HCl	40 ml
(About 90% of the total amount of HCl to be added)		
7	CaCl ₂	0.278 g
8	Na ₂ SO ₄	0.071 g
9	(CH ₂ OH) ₃ CNH ₂	6.057 g
10	Aqua Trides	1 L

2.3 Swelling Ratio

In order to test the swelling ratio, the nano-HA powder was measured at 7.5 mg using an analytical balance. Each sample was then immersed in SBF using a ratio of 1.5mg/ml, then incubated inside an orbital shaker (211DS Shaking Incubator, Labnet, USA) at 120 rpm, with a temperature of 37 °C . The samples were taken out from the solution at various time intervals, which are 24 hours, 48 hours, 7 days, 14 days, and 28 days. To minimize the effect of water weight content at the specified time, the samples were filtrated using filtration paper with sizes of 5–13 µm, and incubated again for 24 hours. The samples were taken out and weighed again with an analytical balance. The swelling ratio was measured using the following formula:

$$\frac{Wt-Wo}{Wo} \times 100\%$$

Wo : initial weight
 Wt : weight after SBF immersion

2.4 pH analysis

The pH of every sample was measured using a pH meter (Orion Star™ A211 Benchtop pH Meter, Thermo Fisher Scientific, USA) after the period mentioned above. The pH of each sample was measured in triplication.

2.5 Fourier Transform Infra-Red (FTIR)

Fourier transform infrared absorption spectra before SBF immersion, seven days, and 28 days after SBF immersion (Nicolet™ iS50 FTIR Spectrometer, Thermo Fisher Scientific, USA) were measured in the spectral range 4000-400 cm^{-1} . Thirty-two scan repetitions were performed for each sample. The results were analyzed using OriginPro2023 (OriginLab Corp., USA)

2.6 Scanning Electromagnetic Microscopy (SEM) - EDX

The sample surface was examined using SEM (FEI Quanta 650 FEG, FEI, USA) and the images were obtained using a voltage of 15 kV with magnifications of 150x, 1000x, and 1500x. Prior to the examination, each sample was coated with gold using a low vacuum sputter coating. Quantitative analyses were made by an electronic dispersive X-ray spectroscopy (EDX) system. Specimens that were observed with SEM were then detected for calcium and phosphorus by shooting X-rays that would produce spectra of elements. The percentage of calcium and phosphorus was converted into a Ca/P ratio. The physical parameters used in EDX are the percentage of weight and atomic elements of the hydroxyapatite.

2.7 Statistical analysis

Statistical analysis was carried out using SPSS version 26 (SPSS Inc, IBM, USA). Values were recorded as means \pm standard deviation and median (min-max). A descriptive statistical analysis was presented.

3. RESULTS AND DISCUSSION

3.1 Swelling Ratio

The bioactivity of an ideal material can be determined not only by its surface morphology and calcium-phosphorus composition but also by its ability to absorb the environmental liquid, which in this study is SBF. The porosity of a material has a significant impact on its absorption properties. The material is more absorbent due to its high porosity percentage. The high percentage of porosity increases the absorbency of the material. High absorption increases cell interaction as well. The absorbed liquid will cause swelling in the cell pores and facilitate cells to infiltrating the scaffold.[18] In this study, we evaluated the swelling properties several times (Figure 1). The n-HA powder is expected to be stable as a scaffold for 14-21 days until cell proliferation is completed.[19] Therefore, in this study, we observed the change in n-HA powder from 24 hours to 28 days following SBF immersion.

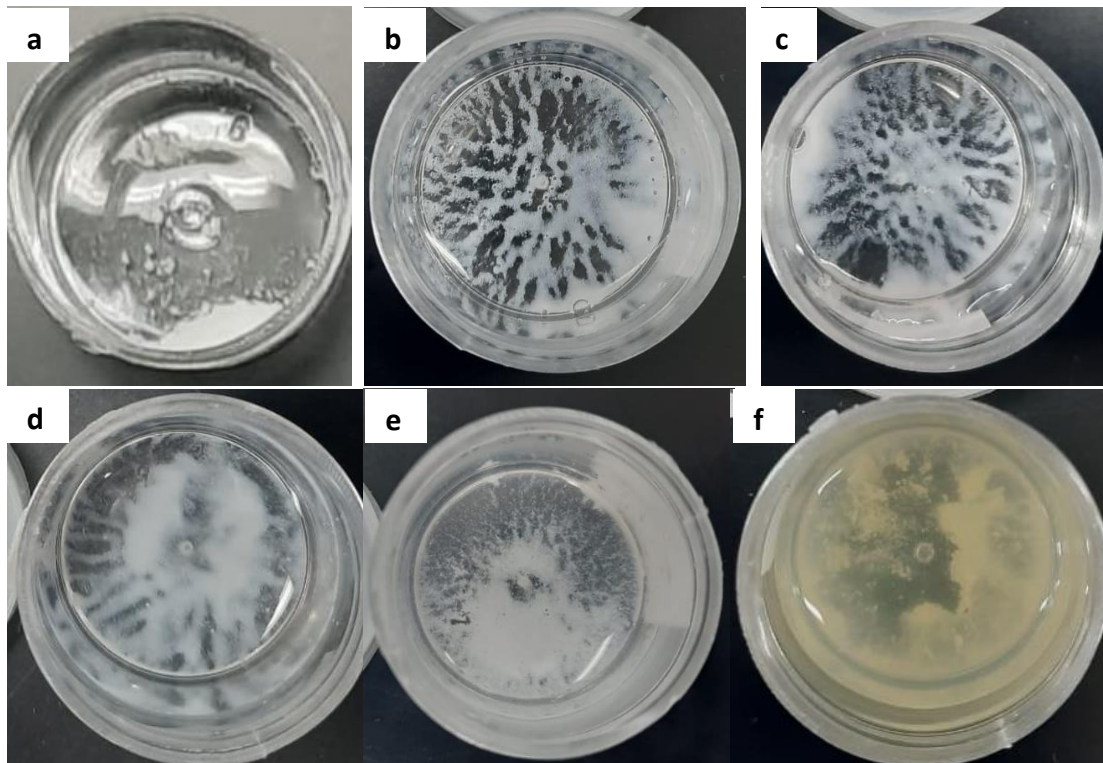


Figure 1 (a) n-HA before immersion, (b) n-HA 24 hours SBF immersion, (c) n-HA 48 hours SBF immersion, (d) n-HA 7-day SBF immersion, (e) n-HA 14-day SBF immersion, (f) n-HA 28 day SBF immersion.

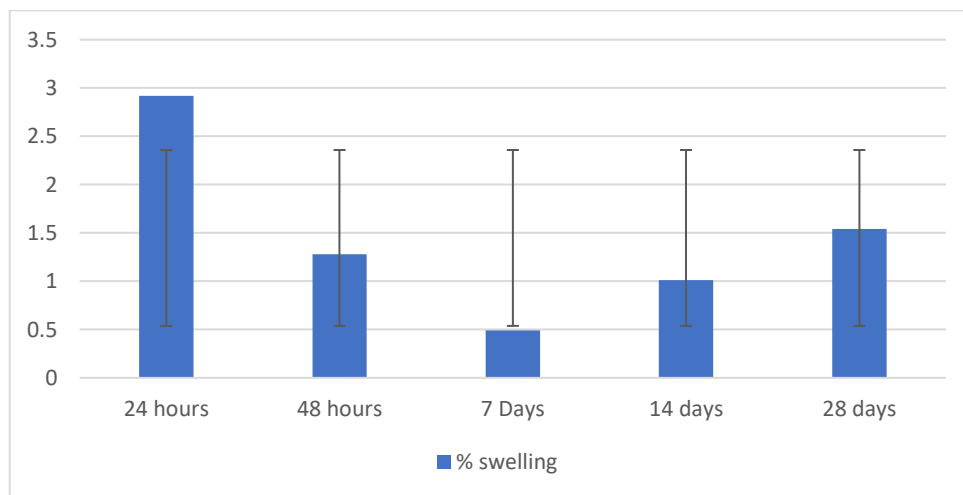


Figure 2 The swelling ratio of n-HA powder in SBF immersion at different times. Statistically significant p-value <0.05 (One-way ANOVA). Number of samples (n) per group: 8

From visual observation, there were changes in the SBF viscosity and color of the 28-day group. Figure 2 shows the mean value of the swelling ratio of nano-HA powder in SBF immersion. The statistical analysis was performed using one-way ANOVA, with a p-value of 0.001 ($p < 0.05$). This

result showed at least some differences among the time groups on the swelling ratio of nano-HA powder in SBF immersion. A post hoc test was performed using Bonferroni because the data was homogenous to determine which group had significant differences. The post hoc test showed significant differences in the swelling ratio between the first 24 hours and other time groups.

A study by Tihan, et al. showed that the higher ratio of HA presented a more hydrophilic character. The hydrophilicity characteristic can determine good cell growth and proliferation. [20] The reaction between nano-HA and physiological fluids can form a strong bond between hard and soft tissue. Nano-HA also has a chemical similarity with the chemical phase of natural bone, increasing the possibility of osseointegration. The nanoscale feature will induce more cellular responses compared with the microscale HA.[21] Therefore, it is known that nano and microtopography can modulate cell behavior, such as cell adhesion, differentiation, and proliferation.[22]

3.2 pH Analysis

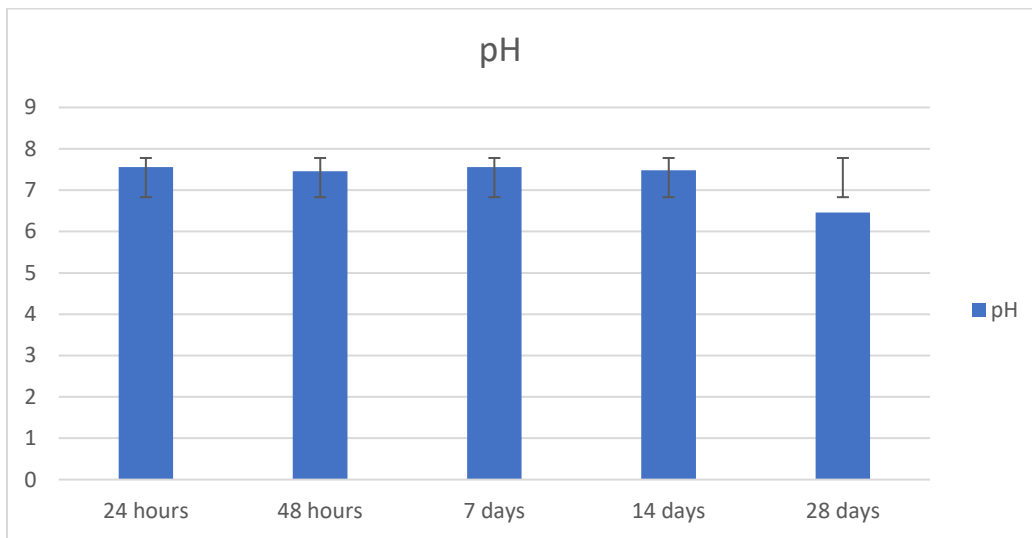


Figure 3 Mean pH value measurement of nano-HA powder in several times. Number of samples (n) per group: 8

Table 3 pH measurement of n-HA powder in several times and statistical significance of the difference in n-HA powder in relation to time groups

Time of SBF Immersion (n=8)	pH Median (Min-Max)	p-value
24h	7.56 (7.53-7.57)	0.001*
48h	7.46 (7.38-7.52)	
7d	7.56 (7.53-7.57)	
14d	7.48 (6.95-7.69)	
28d	6.46 (6.27-6.66)	

Statistically significant p-value < 0.05 (Kruskal Wallis test)

The pH measurement results showed a normal pH from the time of SBF immersion, 24 hours until 14 days. On the 28 days of SBF immersion, the pH decreased. According to statistical analysis using Kruskal-Wallis, the p-value of the pH measurement over time in the SBF immersion group was

0.001 ($p < 0.05$). This result showed that at least there are differences in the pH measurement. The post hoc analysis using the Dunn test was performed and showed significant differences ($p < 0.05$) between a group of 24 hours-48 hours, 24 hour-28 days, 48 hours-7 days, 48 hours-14 days, 48 hours-28 days, 7 days-28 days, and 14 days-28 days. Meanwhile, other groups showed no significant differences in pH measurement.

The SBF's pH trend is constantly stable around 7.4-7.5, except the pH dropped on the 28 days of immersion. The decrease in pH may be due to the partial dissolution of HA.[23] This result may occur from the higher calcium and phosphate contents released into the SBF.[18], [24] The ionic exchange between Ca^{2+} ions from nHA and H^+ ions from SBF may be the cause of the circumstance. Apatite also has an alkaline effect on the pH of SBF; therefore, when the pH is decreasing, then the solubility of HA will increase.[25] The lack of carbonate content of SBF may affect this pH measurement because carbonate act as a pH buffer in blood serum.[26] This current result needs to be confirmed in further research with SBF composition change during the interaction with biomaterials. We also need to remember that there are limitations to in vitro experiments using the SBF to mimic the in vivo conditions of fluid refreshment regimes, local pH, temperature, and endogenous factors.

3.3 Fourier Transform Infra-Red (FTIR)

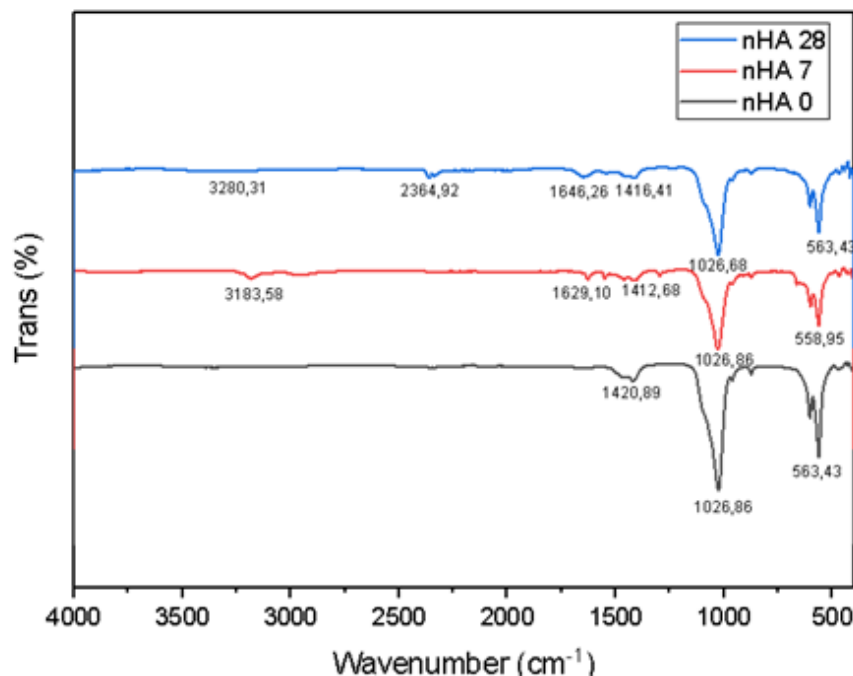


Figure 4 FTIR spectra of n-HA powder before SBF immersion, 7 days of SBF immersion, and 28 days of SBF immersion

Its bend strength characterizes the FTIR of nHA due to the absorption of carbonates and the presence of phosphorus. The FTIR showed a typical spectrum of nano-HA before immersion. The peak band at 530-600 cm^{-1} corresponds to the bending of the PO_4^{3-} functional group. The peak band between 1020-1030 cm^{-1} represents the stretching of the PO_4^{3-} functional group. The peak band at 1415-1420 cm^{-1} was likely associated with a carbonate group (CO_3^{2-}). This peak band can be

observed on the nHA group before SBF immersion at the wavenumbers 563.43 and 1026.86 cm^{-1} for PO_4^{3-} functional group. The peak band of carbonate represents the peak band 1420.89 cm^{-1} .

FTIR spectra of nHA after 7 days of immersion in SBF also showed the phosphate PO_4^{3-} functional group at peak bands 1026.86 and 558.95 cm^{-1} . The peak also showed at 1412.68 cm^{-1} , corresponding to CO_3^{2-} . The absorption band at 3183.58 cm^{-1} showed stretching of the OH group. Meanwhile, the peak at 1629.10 cm^{-1} represents the functional OH and carboxylate groups (COO^-). FTIR spectroscopies of nHA after 28 days of immersion in SBF showed a peak band at 1026.60 and 563.43 cm^{-1} , which refers to the phosphate PO_4^{3-} functional group. It also showed a peak at 1416.41 cm^{-1} corresponding to CO_3^{2-} . The absorption bands at 3280.31 and 2364.92 cm^{-1} showed stretching of the OH group. The peak at 1646.26 cm^{-1} refers to the functional OH group and the carboxylate group (COO^-).

The FTIR spectrum shows the similarity of absorption peaks of functional groups such as PO_4^{3-} . This was because phosphorus compounds often have a robust molecular character regarding their vibrational properties. FTIR before immersion showed a peak band at 563.43 cm^{-1} and after seven days, SBF immersion showed band sharpness at 558.95 cm^{-1} . At 28 days after SBF immersion, band sharpness at 563.43 cm^{-1} , offers reliable evidence of well-crystallized apatite formation. Meanwhile, the FTIR spectrum also showed the absorption peak of functional group CO_3^{2-} on all groups at peak bands 1420.89 cm^{-1} , 1412.68 cm^{-1} , and 1416.41 cm^{-1} , respectively. The functional group CO_3^{2-} represents the presence of nHA. [18] The formation of the carbonate group in the FTIR might result from CO_2 in the atmosphere being dissolved in solution during the synthesis of nano-HA. The carbonate content can also be conserved by the lower calcination temperature.[27]

The adsorbed water in the sample or on the KBr disk was responsible for the broad absorption peak at 1646.62 to 3280.31 cm^{-1} , which occurred in the 28-day SBF immersion groups. This spectrum of the O-H functional groups also showed the hydrolysis ability of the biomaterial.[28]. Hydrolysis occurs due to ion exchange or breaking of molecular chemical bonds from solid to liquid phases, which causes degradation.

3.4 Scanning Electromagnetic Microscopy (SEM) – EDX

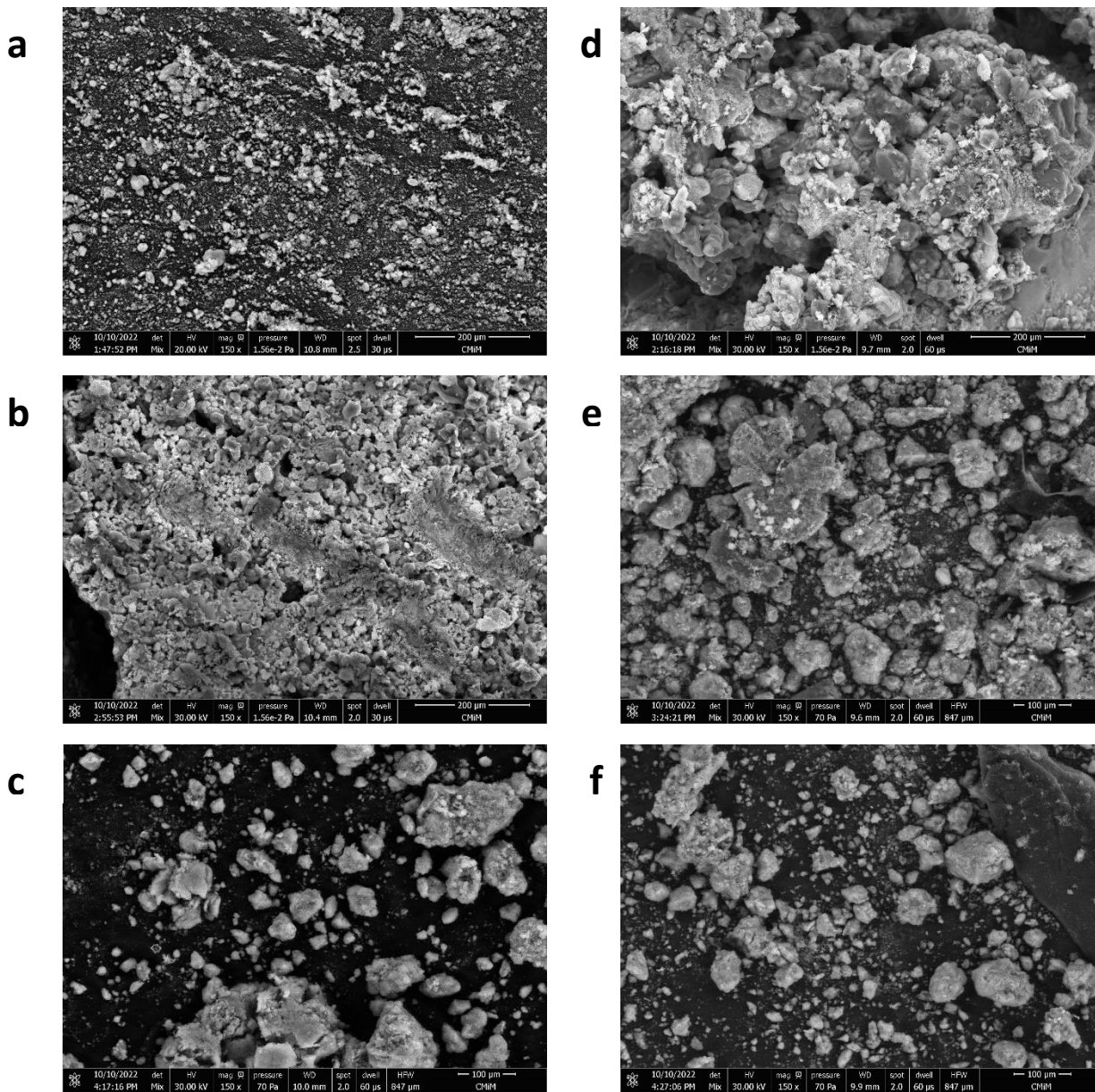


Figure 5 (a) particle shape of n-HA before immersion; (b) particle shape of nano-HA 24 hours SBF immersion; (c) particle shape of n-HA 48 hours SBF immersion; (d) particle shape of n-HA 7 days SBF immersion; (e) particle shape of n-HA 14 days SBF immersion; (f) particle shape of n-HA 28 days SBF immersion.

The result of SEM on the morphology of nano-HA powder is shown in Figure 4. Nano-HA, before immersion in SBF solution, showed irregular globularity with varied sizes, and the surfaces of the irregular structures appeared evenly distributed. The density of particles was high, and no pores were observed on the surface. After 24 hours of immersion in SBF, Nano-HA showed amorphous globular crystals with varied sizes. The characters of globular crystal structures are unevenly distributed, forming three dimensions. The density of particles was high, and pores were observed on the surface. After 48 hours of immersion in SBF, the nano-HA powder revealed an irregular globular of roughly the same size. Compared to the 24-hour group, the surfaces of globular constructions were more equally distributed. High particle densities were found, and regular surface pore observations were made.

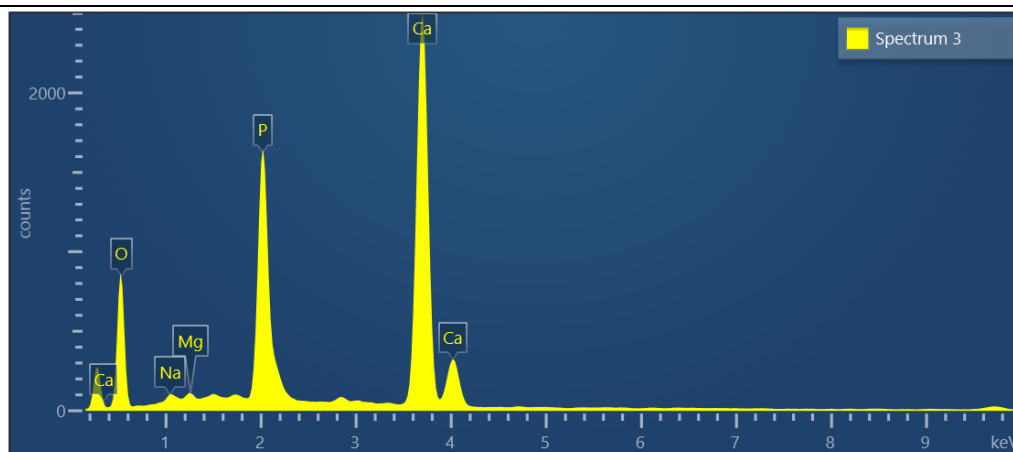
The morphology of nano-HA after 7 days of immersion in SBF solution displayed prominent irregular globular and angular shapes, and the surfaces of the irregular structures appeared evenly distributed. The density of particles was high, and pores were observed on the surface. After 14 days of immersion in SBF solution, nano-HA showed small and large irregular globular crystal shapes, and the surfaces of the irregular structures appeared unevenly distributed. The density of particles was low, and no pores were observed on the surface. Meanwhile, n-HA morphology after 28 days of immersion in SBF solution revealed small and large globular crystals and angular shapes. The surfaces of the irregular structures appeared evenly distributed. The density of particles was low, and no pores were observed on the surface.

Based on the previous study, the morphological difference between before and after immersion of n-HA powder is in the form of globular pores formed due to the accumulation of a new hydroxyapatite layer after immersion in SBF solution.[29] The longer nanohydroxyapatite is immersed in the SBF solution, the more hydroxyapatite layers are formed. A new hydroxyapatite layer is formed due to a large number of mutually attractive particles. Hydroxyapatite can attract calcium ions in the SBF solution so that there is an increase in mineralization and a change in the size and shape of the nanohydroxyapatite.[30]

Porus is formed due to the presence of uneven particles. The size of nano-HA particles also plays a vital role in their interaction with regeneration cells. The size and number of pores increase with the length of the immersion time.[31] Inhibiting cell death, reducing inflammatory activity, and promoting cell proliferation are all benefits of larger-size nano-HA with higher crystallinity. However, cell differentiation benefits could have been more apparent.[22] A study by Ho et al. reported that rod-like nano-HA powder has influenced cell growth and inhibited cell apoptosis.[27]

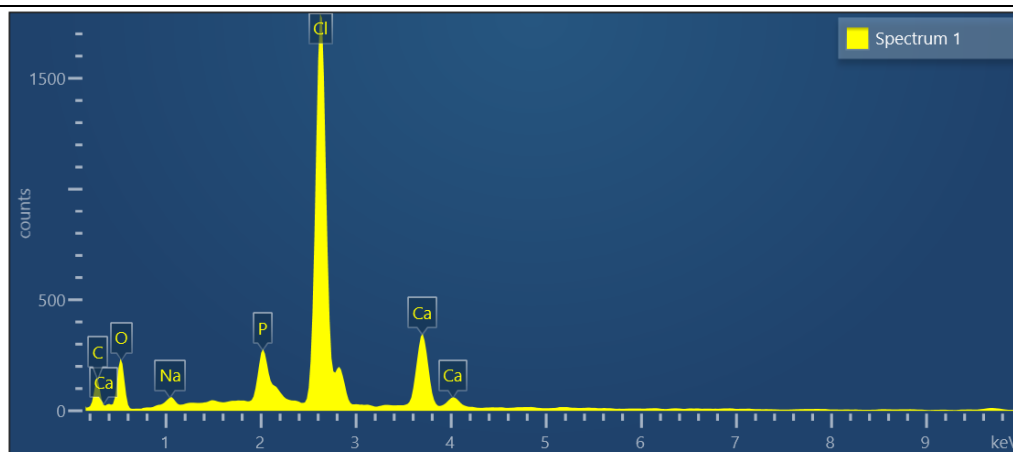
Table 4 Mean Weight Percentage (%) of nano-HA powder pre- and post-SBF immersion

Element	Pre	24h	48h	7d	14d	28d
C	34.23	46.34	42.69	22.01	20.17	25.39
O	51.69	31.68	35.76	36.69	37.29	37.06
P	8.57	1.44	2.38	8.13	11.68	9.57
Ca	16.15	3.39	5.03	17.84	27.27	19.29
Mg	0.56	-	-	0.74	-	0.14
Na	0.89	0.96	-	5.14	1.09	2.52
Cl	-	16.89	13.99	9.19	1.32	5.51
Al	-	-	0.25	0.43	1.18	0.43
K	-	-	-	0.32	-	0.26



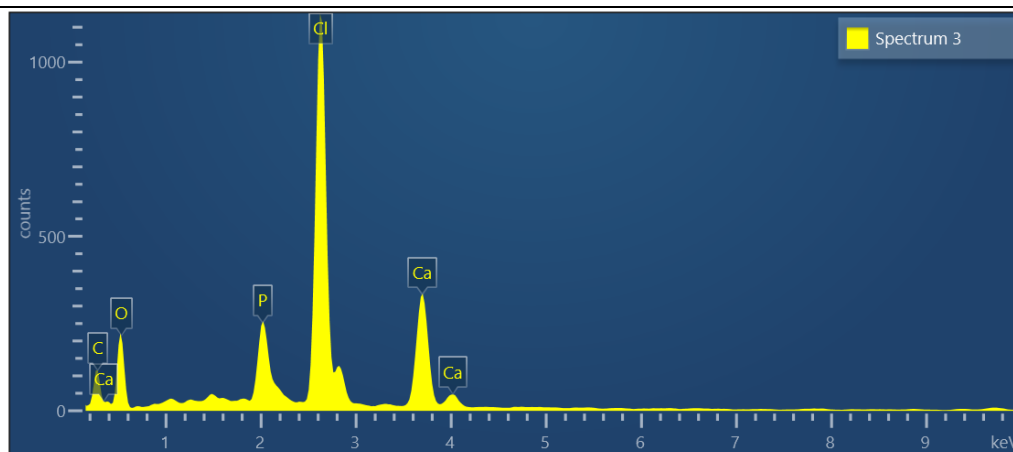
Element	Wt%	At%
C K	-	-
O K	63.08	0.69
NaK	1.04	0.29
MgK	0.75	0.18
Al K	-	-
Si K	-	-
P K	12.14	0.30
Ca K	23.00	0.45

Pre



Element	Wt%	At%
C K	46.99	2.59
O K	30.31	1.85
NaK	0.89	0.20
MgK	-	-
Al K	-	-
Cl K	15.80	0.81
P K	1.87	0.15
Ca K	4.15	0.25

24h



Element	Wt%	At%
C K	42.86	55.66
O K	36.07	35.17
NaK	-	-
MgK	-	-
Al K	-	-
Cl K	13.38	5.89
P K	2.49	1.25
Ca K	5.20	2.02

48h

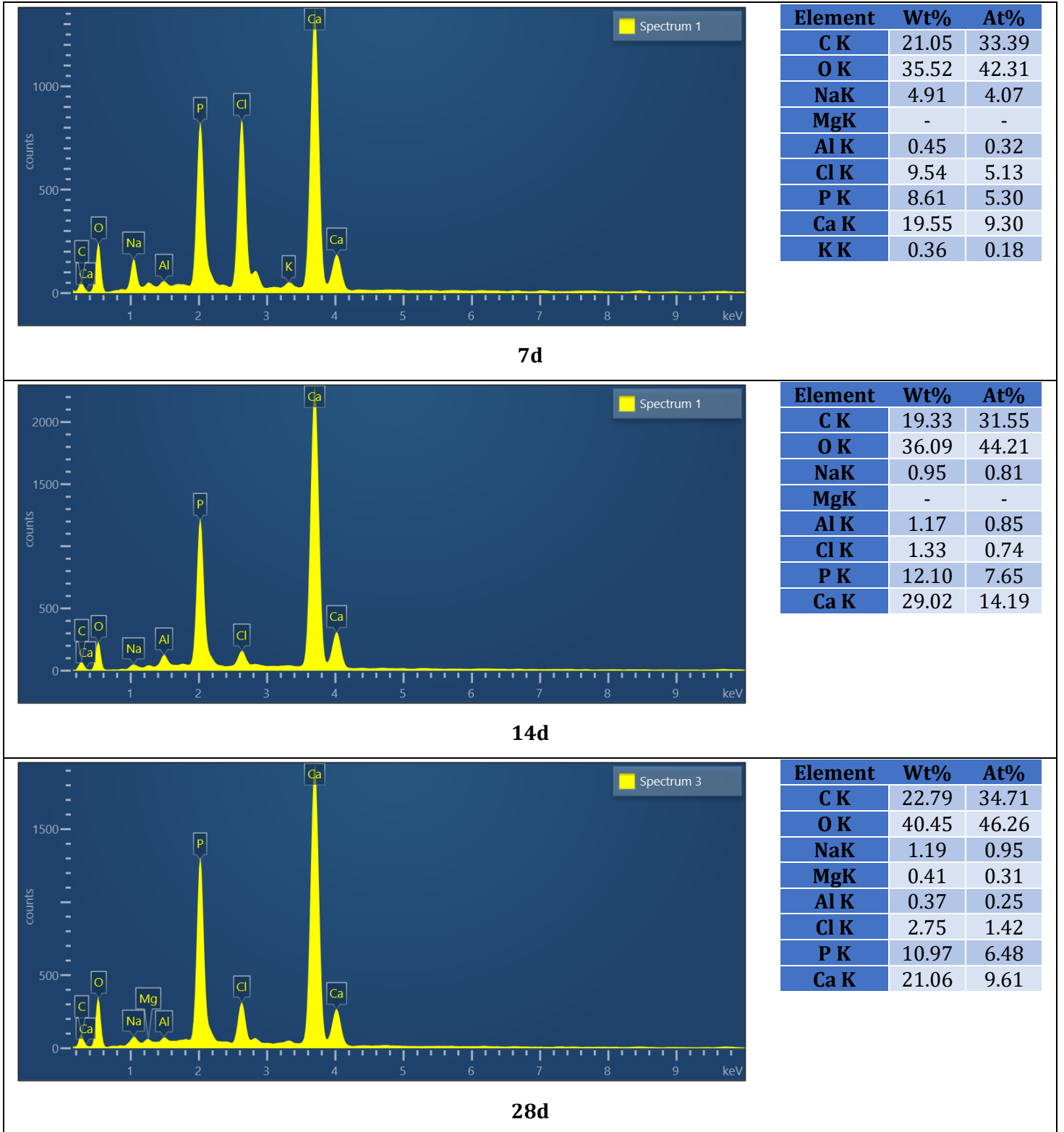


Figure 6 EDX spectra of n-HA pre-immersion, 24h, 48h, 7d, 14d and 28d

Each sample was examined with three spectra EDX and the spectrums shown in the Figure 5 were the spectrum with the highest concentration of Ca. Table 4 shows the average concentration of ions at each immersion period.

Table 5 Ca/P Ratio of nano-HA powder pre- and post-SBF immersion

Time of SBF Immersion	Ca/P Ratio Median (Min-Max)	p-value
Pre	1.93 (1.81-2.00)	0.015*
24h	2.26 (2.22-2.82)	
48h	2.09 (2.02-2.24)	
7d	2.18 (2.12-2.27)	
14d	2.31 (2.30-2.40)	
28d	2.07 (1.92-2.07)	

Statistically significant p-value < 0.05 (Mann Whitney-U test)

Kruskal-Wallis analysis showed the p-value of the Ca/P ratio was 0.015 ($p < 0.05$). This result showed at least some differences in the Ca/P ratio according to the time of SBF immersion. Therefore, the post hoc test was performed using Mann Whitney-U to analyze the significant differences between groups. The post hoc test showed significant differences ($p < 0.05$) in group 28 days of SBF immersion compared to groups after 24 hours, 7 days, and 14 days of SBF immersion. Ion exchange between biomaterial and SBF will occur during the immersion of biomaterial. The Ca/P ratio will determine the bioactivity of biomaterials, whereas a high Ca/P marked as bioactive and a lower Ca/P ratio will disrupt the binding of biomaterials to the bone. Some minerals were also found in either pre or post-SBF immersion, such as Mg, Na, Cl, Al, and K. In the initial phase of the hydroxyapatite-like layer, there will be an exchange of H^+ ions from the SBF, releasing Ca^{2+} , Mg^{2+} , and Na^+ ions into the SBF solution.[18], [24] The use of SBF in this study also played a significant role because, unlike blood serum, SBF is devoid of proteins. Proteins are known to control apatite nucleation as inhibitors. Therefore, SBF can only precipitate hydroxyapatite at physiological temperatures.[26]

4. Conclusion

In our study, the nano-HA powder was confirmed to have hydrophilic properties and showed an excellent chemical composition by finding the carbonate and phosphate functional groups. FTIR assays on n-HA powders identify functional groups PO_3^- , CO_2 -O-H, C=H, and COO. The elemental composition as determined by EDX indicated the transformation of calcium phosphate into apatite with the increase of the Ca/P ratio during the SBF immersion. Even though the pH measurement was relatively stable until 14 days, we still detected depression after 28 days of SBF immersion. Therefore, further investigation is required to confirm the toxicity and cell response of the n-HA powder as a bone graft material.

5. Conflict of Interests

The authors declare no conflict of interest in conducting this research.

6. Funding Research

This research is funded by [SIMLITABMAS Penelitian Dasar Unggulan Perguruan Tinggi (PDUPT)] (Grant No. 5/E5/PG.02.00.PT/2022) to Yuniarti Soeroso, Nadhia Anindhita Harsas, and Endang Winiati Bachtiar.

7. References

- [1] Poinern, G. E., Brundavanam, R. K., Mondinos, N., and Jiang, Z. T. Synthesis and characterisation of nanohydroxyapatite using an ultrasound assisted method. *Ultrason Sonochem.* vol **16**, no. 4 (2009) pp. 469–474 doi: 10.1016/j.ultsonch.2009.01.007.
- [2] Xu, A., Zhou, C., Qi, Wi., and He, F. Comparison Study of Three Hydroxyapatite-Based Bone Substitutes in a Calvarial Defect Model in Rabbits. *Int J Oral Maxillofac Implants.* vol **34**, no. 2 (2019) pp. 434–442. doi: 10.11607/jomi.7174.
- [3] Yamada, S., Shanbhag, S., and Mustafa, K. Scaffolds in Periodontal Regenerative Treatment. *Dental Clinics of North America.* vol **66**, no. 1 (2022) pp. 111–130. doi: 10.1016/j.cden.2021.06.004.
- [4] Pérez-Sayáns, M., et al. Evaluation of a new tricalcium phosphate for guided bone regeneration: an experimental study in the beagle dog. *Odontology.* vol **107**, no. 2 (2019) pp. 209–218. doi: 10.1007/s10266-018-0384-z.
- [5] Bayani, M., Torabi, S., Shahnaz, A., and Pourali, M. Main properties of nanocrystalline hydroxyapatite as a bone graft material in treatment of periodontal defects. A review of literature. *Biotechnology and Biotechnological Equipment.* vol **31**, no. 2 (2017) pp. 215–220. doi: 10.1080/13102818.2017.1281760.
- [6] Pepla, E., Besharat, L. K., Palaia, G., Tenore, G., and Migliau, G. Nano-hydroxyapatite and its applications in preventive, restorative and regenerative dentistry: a review of literature. *Ann Stomatol (Roma).* vol **5**, no. 3 (2015) pp. 108–114.
- [7] Rana, Md. M., Akhtar, Md. N., Rahman, Md. S., Hasan, Z., and Asaduzzaman, S. M. Extraction and characterization of hydroxyapatite from bovine cortical bone and effect of radiation. *International Journal of Biosciences (IJB).* vol **11**, no. 3 (2017) pp. 20–30. doi: 10.12692/ijb/11.3.20-30.
- [8] Abere, D. V., Ojo, S. A., Oyatogun, G. M., Paredes-Epinosa, M. B., Niluxsshun, M. C. D., and Hakami, A. Mechanical and morphological characterization of nano-hydroxyapatite (nHA) for bone regeneration: A mini review. *Biomedical Engineering Advances.* vol **4**, (2022) p. 100056. doi: 10.1016/j.bea.2022.100056.
- [9] O'Neill, E., Awale, G., Daneshmandi, L., Umerah, O., and Lo, K. W. H. The roles of ions on bone regeneration. *Drug Discovery Today.* vol **23**, no. 4 (2018) pp. 879–890 doi: 10.1016/j.drudis.2018.01.049.
- [10] Hulla, J. E., Sahu, S. C., and Hayes, A. W. Nanotechnology: History and future. *Human and Experimental Toxicology.* vol **34**, no. 12 (2015) pp. 1318–1321. doi: 10.1177/0960327115603588.
- [11] Ryabenkova, Y., Mobus, G., Quadros, P. A., and Crawford, A. The relationship between particle morphology and rheological properties in injectable nano-hydroxyapatite bone

- graft substitutes. *Materials Science and Engineering C*. vol **75**, (2017) pp. 1083–1090. doi: 10.1016/j.msec.2017.02.170.
- [12] Alharith, D., Al-Omari, M., Almnea, R., Basri, R., Alshehri, A., and Al-Nufiee, A. Clinical efficacy of single application of plain nano-hydroxyapatite paste in reducing dentine hypersensitivity - A randomized clinical trial. *Saudi Endodontic Journal*. vol **11**, no. 1 (2021) pp. 24–30. doi: 10.4103/sej.sej_46_20.
- [13] Dridi, A., Riahi, K. Z., and Somrani, S. Mechanism of apatite formation on a poorly crystallized calcium phosphate in a simulated body fluid (SBF) at 37 °C. *Journal of Physics and Chemistry of Solids*. vol **156**, (2021) pp. 1-14. doi: 10.1016/j.jpcs.2021.110122.
- [14] Kim, H. M., Himeno, T., Kawashita, M., Kokubo, T., and Nakamura, T. The mechanism of biomineralization of bone-like apatite on synthetic hydroxyapatite: An in vitro assessment. *J R Soc Interface*. vol **1**, no. 1 (2004) pp. 17–22. doi: 10.1098/rsif.2004.0003.
- [15] Kokubo, T and Takadama, H. How useful is SBF in predicting in vivo bone bioactivity? *Biomaterials*. vol **27**, no. 15 (2006) pp. 2907–2915. doi: 10.1016/j.biomaterials.2006.01.017.
- [16] Polidar, M., Metzsch-Zilligen, E., and Pfaendner, R. Controlled and Accelerated Hydrolysis of Polylactide (PLA) through Pentaerythritol Phosphites with Acid Scavengers. *Polymers (Basel)*. vol **14**, no. 19 (2022) pp. 1-19. doi: 10.3390/polym14194237.
- [17] Kokubo, T and Yamaguchi, S. Simulated body fluid and the novel bioactive materials derived from it. *Journal of Biomedical Materials Research - Part A*. vol **107**, no. 5 (2019) pp. 968–977. doi: 10.1002/jbm.a.36620.
- [18] Araújo, M., Miola, M., Baldi, G., Perez, J., and Verné, E. Bioactive glasses with low Ca/P ratio and enhanced bioactivity. *Materials*. vol **9**, no. 4 (2016) doi: 10.3390/ma9040226.
- [19] Bitar, K. N., and Zakhem, E. Design Strategies of Biodegradable Scaffolds for Tissue Regeneration. *Biomed Eng Comput Biol*. vol **6**, (2014) p. BECB.S10961. doi: 10.4137/beceb.s10961.
- [20] Tihan, T. G., Ionita, M. D., Popescu, R. G., and Iordachescu, D. Effect of hydrophilic-hydrophobic balance on biocompatibility of poly(methyl methacrylate) (PMMA)-hydroxyapatite (HA) composites. *Materials Chemistry and Physics*. vol **118**, no. 2–3 (2009) pp. 265–269. doi: 10.1016/j.matchemphys.2009.03.019.
- [21] Yousefi, A. M., Oudadesse, H., Akhbarzadeh, R., Wers, E., and Lucas-Girot, A. A review of calcium phosphate cements and acrylic bone cements as injectable materials for bone repair and implant fixation. *J Appl Biomater Funct Mater*. vol **17**, no. 4 (2019). doi: 10.1177/2280800019872594.
- [22] Liu, X., Zhao, M., Lu, J., Ma, J., Wei, J., and Wei, S. Cell responses to two kinds of nanohydroxyapatite with different sizes and crystallinities. *Int J Nanomedicine*. vol **7**, (2012) pp. 1239–1250. doi: 10.2147/IJN.S28098.
- [23] Cortés, D.A., Medina, A., Escobedo, S., and López, M. A. Biomimetic apatite formation on a CoCrMo alloy by using wollastonite, bioactive glass or hydroxyapatite. *J Mater Sci*. vol **40**, no. 13 (2005) pp. 3509–3515. doi: 10.1007/s10853-005-2856-0.
- [24] Habibovic, P. In vitro and in vivo bioactivity assessment of a polylactic acid/hydroxyapatite composite for bone regeneration. *Biomatter*. vol **4**, (2014) p. e27664. doi: 10.4161/biom.27664.
- [25] Minouei, H., Fathi, M., Meratian, M., and Ghazvinizadeh, H. Heat Treatment Of Cobalt-Base Alloy Surgical Implants With Hydroxyapatite-Bioglass For Surface Bioactivation. *Iranian Journal of Material Science & Engineering*. vol **9**, no. 3 (2012) pp. 33-39.

- [26] Baino, F., and Yamaguchi, S. The use of simulated body fluid (SBF) for assessing materials bioactivity in the context of tissue engineering: Review and challenges. *Biomimetics*. vol **5**, no. 4 (2020) pp. 1–19. doi: 10.3390/biomimetics5040057.
- [27] Ho, K. H. L., Dao, V. H., Pham, X. K., et al. Physicochemical properties, acute and subchronic toxicity of nano-hydroxyapatite obtained from *Lates calcarifer* fish bone. *Reg Stud Mar Sci*. vol **55**, no. 102560 (2022) pp 1-10. doi: 10.1016/j.rsma.2022.102560.
- [28] Kaygili, O., Keser, S., Kom, M., Bulut, N., and Dorozhkin, S. V. The effect of simulating body fluid on the structural properties of hydroxyapatite synthesized in the presence of citric acid. *Prog Biomater*. vol **5**, no. 3-4 (2016) pp. 173–182. doi: 10.1007/s40204-016-0055-5.
- [29] Nguyen, N. K., Leoni, M., Maniglio, D., and Migliaresi, C. Hydroxyapatite nanorods: Soft-template synthesis, characterization and preliminary *in vitro* tests. *J Biomater Appl*. vol **28**, no. 1 (2013) pp. 49–61. doi: 10.1177/0885328212437065.
- [30] Chavan, P. N., Bahir, M. M., Mene, R. U., Mahabole, M. P., and Khairnar, R. S. Study of nanobiomaterial hydroxyapatite in simulated body fluid: Formation and growth of apatite. *Materials Science and Engineering: B*. vol **168**, no. 1–3 (2010) pp. 224–230. doi: 10.1016/j.mseb.2009.11.012.
- [31] Kong, L., Gao, Y., Lu, G., Gong, Y., Zhao, N., and Zhang, X. A study on the bioactivity of chitosan/nano-hydroxyapatite composite scaffolds for bone tissue engineering. *Eur Polym J*. vol **42**, no. 12 (2006) pp. 3171–3179. doi: 10.1016/j.eurpolymj.2006.08.009.

